Natural variation in a molybdate transporter controls grain molybdenum concentration in rice

Xin-Yuan Huang[1,*], Huan Liu[1], Yu-Fei Zhu[1], Shannon R M Pinson[2], Hong-Xuan Lin[3], Mary Lou Guerinot[4], Fang-Jie Zhao[1], David E Salt[5,*]

[1]State Key Laboratory of Crop Genetics and Germplasm Enhancement, College of Resources and Environmental Sciences, Nanjing Agricultural University, Nanjing 210095, China

[2]USDA–ARS Dale Bumpers National Rice Research Center, Stuttgart, AR 72160 USA

[3]National Key Laboratory of Plant Molecular Genetics, CAS Centre for Excellence in Molecular Plant Sciences and Collaborative Innovation Center of Genetics & Development, Shanghai Institute of Plant Physiology & Ecology, Shanghai Institute for Biological Sciences, Chinese Academic of Sciences, Shanghai 200032, China

[4]Department of Biological Sciences, Dartmouth College, Hanover, New Hampshire 03755, USA

[5]School of Biosciences, University of Nottingham, Sutton Bonington Campus, Loughborough, Leicestershire LE12 5RD, UK

[*]Authors for Correspondence:

Xin-Yuan Huang

Tel: +86 2584399562

Email: xinyuan.huang@njau.edu.cn

David E Salt

Tel: +44 1159516339

Email: david.salt@nottingham.ac.uk

Total word count (excluding summary, references and legends):	6764	No. of figures:	8 (Figs 1- 8 in color)
Summary:	198	No. of Tables:	0
Introduction:	859	No of Supporting Information files:	11 (Fig. S1-S8; Table S1-S2; Methods S1)
Materials and Methods:	1504		
Results:	2846		
Discussion:	1409		
Acknowledgements:	107		

1

Summary

- Molybdenum (Mo) is an essential micronutrient for most living organisms, including humans. Cereals such as rice are the major dietary source of Mo. However, little is known about the genetic basis of the variation in Mo content in rice (*Oryza sativa* L.) grain.
- We mapped a quantitative trait locus (QTL) *qGMo8* that controls Mo accumulation in rice grain by using a recombinant inbred line population and a backcross introgression line population.
- We identified a molybdate transporter, *OsMOT1;1*, as the causal gene for this QTL. OsMOT1;1 exhibits transport activity for molybdate, but not sulfate, when heterogeneously expressed in yeast cells. *OsMOT1;1* is mainly expressed in roots and is involved in the uptake and translocation of molybdate under molybdate limited condition. Knock-down of *OsMOT1;1* results in less Mo being translocated to shoots, lower Mo concentration in grains and higher sensitivity to Mo deficiency. We reveal that the natural variation of Mo concentration in rice grains is attributed to the variable expression of *OsMOT1;1* due to sequence variation in its promoter.
- Identification of natural allelic variation in *OsMOT1;1* may facilitate the development of rice varieties with Mo enriched grain for dietary needs and improve Mo nutrition of rice on Mo-deficient soils.

Key words: molybdenum, mineral nutrient, natural variation, QTL, rice

Introduction

As one of the most important staple crops, rice not only provides more than one fifth of daily calories for half of the world's human population but is also a major source of mineral nutrients such as Mo, an essential micronutrient for almost all living organisms. In humans, Mo is required for the biosynthesis of molybdenum cofactor (Moco), which forms the active site of molybdenum-requiring enzymes (molybdoenzymes) including aldehyde oxidase, xanthine dehydrogenase, sulfite oxidase and amidoxime reducing component (Schwarz & Mendel, 2006). These enzymes participate in crucial processes such as purine metabolism and sulfite detoxification and play a vital role in maintaining human health (Schwarz & Mendel, 2006). Deficiency of Moco biosynthesis in humans results in the decrease of molybdoenzyme activity, which leads to inheritable progressive neurological damage and even early childhood death (Johnson *et al.*, 1980; Schwarz, 2005). Although Mo deficiency in humans is extremely rare, food crops grown on soils that are freely drained, acidic and rich in iron oxides are known to have lower Mo concentrations (Marschner & Rengel, 2012).

Mo is also an essential micronutrient for plants. Plants take up Mo mainly as molybdate. Molybdate itself is biologically inactive and must be incorporated into tricyclic pterin to form Moco. Moco serves as electron donors and/or acceptors in molybdoenzymes and plays key roles in the assimilation and biogeochemical cycles of carbon, nitrogen, and sulfur (Schwarz & Mendel, 2006; Bittner, 2014). Although Mo deficiency in humans is rare, Mo deficiency in crops is becoming an agricultural problem, especially for crops grown on acid soils. In acid soils, the high levels of reactive iron oxides/hydroxides are known to have a strong adsorption of molybdate which deceases the bioavailability of Mo (Marschner & Rengel, 2012). It is estimated that up to 70% of the world's arable is characterized acidic, Mo deficiency is thus a widespread agricultural concern (von Uexküll & Mutert, 1995). The deficiency of Mo in soils has been shown to inhibit plant growth and agricultural productivity (Kaiser *et al.*, 2005). Plants suffering from Mo deficiency develop the typical "whiptail" phenotypes, which includes mottled lesions on the leaves, rolling of leaves and wilting of leaf edges (Arnon & Stout, 1939).

Living organisms that require Mo to synthesize molybdoenzymes take up Mo from the environment in an energy dependent process. In *Escherichia coli*, Mo is taken up by a high-affinity ABC-type transport system. This system is encoded by *modABC* genes and composed of a periplasmic molybdate-binding protein (ModA), a membrane channel protein (ModB), and an energy-transducing ATPase protein (ModC) (Grunden & Shanmugam, 1997; Hollenstein *et al.*, 2007). A large number of ABC transporter genes are present in the genome of eukaryotes; however, none of the ABC-type Mo-specific transporters have been identified in eukaryotes (Kaiser *et al.*, 2005). The first eukaryotic high-affinity molybdate transporter encoded by *MoT1* (*CrMOT1*) was identified in the green alga *Chlamydomonas reinhardtii* (Tejada-Jimenez *et al.*, 2007). Knock-down of *CrMOT1* by an antisense RNA strategy inhibited the molybdate transport activity and the activity of the Mo-containing enzyme nitrate reductase, indicating a function of CrMOT1 in molybdate transport (Tejada-Jimenez *et al.*, 2007). A high-affinity molybdate transporter AtMOT1;1 (also named as MOT1) that shows sequence similarity to CrMOT1 was also identified in *Arabidopsis thaliana* (Tomatsu *et al.*, 2007; Baxter *et al.*, 2008). *AtMOT1;1* belongs to group V of the sulfate transporter superfamily and was previously named as *Sultr5;2* (Tejada-Jimenez *et al.*, 2013). Knock-out of *AtMOT1;1* led to decreased accumulation of Mo in both roots and shoots and the *atmot1;1* mutant showed Mo deficiency symptoms when grown under limited Mo supply conditions, suggesting an essential role of *AtMOT1;1* in uptake of Mo from soil in *A. thaliana* (Tomatsu *et al.*, 2007; Baxter *et al.*, 2008). Another member of group V of the sulfate transporter superfamily, *AtMOT1;2* (*Sultr5;1*; previously named *MOT2*), was also identified in *A. thaliana*, which localizes to the tonoplast and functioned in vacuolar molybdate export (Gasber *et al.*, 2011). Recently, *LjMOT1* was isolated from *Lotus japonicus*, which is essential for *L. japonicus* to take up Mo from the soil (Gao *et al.*, 2016; Duan *et al.*, 2017). Very recently, *MtMOT1.3* was identified in the model legume *Medicago truncatula*, which is required for nitrogenase activity in root nodules (Tejada-Jimenez *et al.*, 2017). In *C. reinhardtii*, there is another molybdate transporter CrMOT2, which shows no sequence similarity to CrMOT1 and thus is not related to the MOT1 family (Tejada-Jimenez *et al.*, 2011). CrMOT2 is also a high-affinity molybdate transporter and mainly functions under the molybdate deficient

conditions (Tejada-Jimenez *et al.*, 2011). To date, molybdate transporters that control Mo concentration have not been characterised in staple food crops.

In this study, we identify a quantitative trait locus (QTL) *qGMo8* that controls the variation in grain Mo concentration in rice. We show that *qGMo8* encodes a molybdate transporter OsMOT1;1. *OsMOT1;1* is mainly expressed in roots and exhibits molybdate transport activity when heterogeneously expressed in yeast cells. Loss-of-function of *OsMOT1;1* results in decreased Mo translocation from roots to shoots, lower Mo concentration in grains and higher sensitivity to Mo deficiency. We further reveal that the natural variation of Mo concentration in rice grains is attributed to the variable expression of *OsMOT1;1* in roots.

Materials and Methods

Plant materials and growth conditions

The rice (*Oryza sativa* L.) recombinant inbred lines derived from a cross between Lemont (LM, *japonica*) and TeQing (TQ, *indica*) (LT-RILs), and TeQing-into-Lemont backcross introgression lines (TILs) were described previously (Tabien *et al.*, 2000; Pinson *et al.*, 2012; Huang *et al.*, 2016b). The heterogeneous inbred families (HIFs) of *OsMOT1;1* locus were generated as previously described (Tuinstra *et al.*, 1997; Loudet *et al.*, 2005). A PCR marker was developed based on the 222 bp deletion in the promoter of *OsMOT1;1* in TQ, and was used for genotyping the TILs. The line TIL669.4 was determined to be heterozygous at the *OsMOT1;1* locus. Plants fixed with TQ allele (HIF669.4-TQ) and plants fixed with Lemont allele (HIF669.4-LM) were identified in the next generation of TIL669.4, resulting in HIFs for comparing phenotypic effects of the *OsMOT1;1* alleles from TQ and LM. The T-DNA insertion mutant for *OsMOT1;1* which is in Zhonghua 11 background was obtained from Huazhong Agricultural University, China (http://rmd.ncpgr.cn). The segregated plants without T-DNA insertion in *OsMOT1;1* gene were used as a WT control. The WT and T-DNA seeds were planted into soil in a greenhouse at the University of Aberdeen, U.K., or hydroponically grown in Nanjing Agricultural University, China. The *A. thaliana* T-DNA insertion mutant for *AtMOT1;1*

(SALK_118311) was obtained from the Arabidopsis Biological Resource Center (ABRC, http://www.arabidopsis.org/abrc/).

The growth of LT-RIL and TIL populations in the field in Texas, U.S.A., and the growth of the TIL population in a greenhouse in Purdue University were described previously (Zhang *et al.*, 2014; Huang *et al.*, 2016b). For analysis of the grains and different tissues of the WT and *osmot1;1*, plants were grown in soil in a greenhouse at the University of Aberdeen, U.K. as described previously (Huang *et al.*, 2016b). For the hydroponic experiment, WT and *osmot1;1* plants were grown in 96-well plates with the bottom removed. The plates were put in tip boxes containing half-strength Kimura B solution with different concentrations of Mo. The growth condition was described previously (Huang *et al.*, 2016b). *A. thaliana* transgenic plants were grown on MGRL agar media in a growth chamber at the University of Aberdeen, U.K. as described (Huang *et al.*, 2016a).

QTL analysis and fine mapping of *qGMo8*

The QTL mapping has been performed previously by using both multiple interval mapping (MIM) and Bayesian information criterion (BIC) methods based on the least squares (LS) means of the 5 years-replications for the grain Mo of LT-RIL and three replications of TIL (Zhang *et al.*, 2014). We reperformed QTL analyses based on the individual year data under flooded or unflooded field conditions by using Windows QTL cartographer version 2.5 (http://statgen.ncsu.edu/qtlcart/WQTLCart.htm) with a composite interval mapping (CIM) method according to previous studies (Huang *et al.*, 2016b). Seven markers were developed in the *qGMo8* mapping interval and used to genotype the entire population of 123 TILs. Three representative TILs with different genotypes in the *qGMo8* mapping interval and two control TILs were chosen for further replicated phenotypic analyses and fine mapping. By integration of the genotypes and grain Mo concentrations of these lines, the *qGMo8* was fine mapped to a 522 kb region on the top of chromosome 8. The primer sequences are listed in Table S2.

Tissue elemental analysis

The elemental concentrations in grains of LT-RILs, TILs, WT and *osmot1;1* were determined using an inductively couple plasma mass spectrometer (ICP-MS, Elan DRCe, PerkinElmer; or NexION 300D, PerkinElmer) according to previous studies (Zhang *et al.*,

2014; Huang *et al.*, 2016b). For determination of elemental concentrations in different organs of WT and *osmot1;1* grown in soil, tissues were excised and washed with Milli-Q water and dried at 88°C overnight. For analysis of roots of WT and *osmot1;1* grown hydroponically, roots were excised and washed with 0.5 mM $CaCl_2$ solution three times and rinsed with Milli-Q water once and then dried at 88°C overnight. Samples were digested with concentrated HNO_3 at 118°C for 4 h. The elemental concentrations in the digested samples were determined by ICP-MS (Huang *et al.*, 2016b). The Mo concentrations in shoots and roots of transgenic *A. thaliana* plants were determined according to previous studies (Huang *et al.*, 2016a).

Genetic and transgenic complementation test

For genetic complementation, *osmot1;1* as well as WT T-DNA progeny were crossed with HIF669.4-TQ and HIF669.4-LM, respectively. The concentrations of Mo in grains of F1 plants from each cross were then determined. For transgenic complementation, the full-length coding sequence of *OsMOT1;1* was PCR amplified using the cDNA of TQ or LM as templates. The correct PCR fragments confirmed by sequencing were ligated into the *Sal*I-*Spe*I site of p1301GFP vector (Huang *et al.*, 2009) to generate the *35S:OsMOT1;1(TQ)-GFP* and *35S:OsMOT1;1(LM)-GFP* constructs. The resulting plasmids were transformed into *Agrobacterium tumefaciens* strain HA105 and introduced into rice *japonica* cv. Zhonghua 11 as described previously (Hiei *et al.*, 1994). *osmot1;1* was crossed with two transgenic *OsMOT1;1* overexpression lines, *35S:OsMOT1;1(TQ)-GFP* and *35S:OsMOT1;1(LM)-GFP*. Two independent transgenic lines of *35S:OsMOT1;1(TQ)-GFP* and *35S:OsMOT1;1(LM)-GFP* were used for crossing. In subsequent F_2 populations, plants containing the transgene in homozygous *osmot1;1* mutant background were identified by genotyping. Plants without the transgene in WT or homozygous *osmot1;1* mutant background were used as controls. The grain Mo concentrations in grains from these F2 plants were determined by ICP-MS. The primer sequences using for genotyping are listed in Table S2.

Expressing *OsMOT1;1* in an *A. thaliana atmot1;1* mutant

OsMOT1;1 was expressed in an *A. thaliana atmot1;1* T-DNA mutant using the 35S promoter or *AtMOT1;1* native promoter. The construction of *35S:OsMOT1;1(TQ)-GFP*

and *35S:OsMOT1;1(LM)-GFP* vectors was as described above. To generate the *AtMOT1;1* promoter driven *OsMOT1;1* expression vectors, the 1,777-bp promoter sequence of *AtMOT1;1* was PCR amplified from the genomic DNA of Col-0 using the primers listed in Table S2. The PCR fragment confirmed by sequencing was used to substitute the 35S promoters in the *35S:OsMOT1;1(TQ)-GFP* and *35S:OsMOT1;1(LM)-GFP* vectors to generate *MOT1pro:OsMOT1;1(TQ)-GFP* and *MOT1pro:OsMOT1;1(LM)-GFP* vectors, respectively. These plasmids were also transformed into *Agrobacterium tumefaciens* strain GV3101 and introduced in *A. thaliana mot1* mutant (SALK_118311) using the floral dip method (Clough & Bent, 1998). To assay low pH sensitivity, homozygous T3 transgenic plants were grown on MGRL medium with Mo omitted. The low pH media was prepared as described above by adding 35 µl 6 M HCl into 100 ml media after autoclaving. Plants were grown on plates horizontally in a climate-controlled room with temperature of 19-22°C, photoperiod of 10 h light (100 ± 10 µmol m^{-2} s^{-1})/14 h dark and humidity of 60%. The shoots were weighed after growing for 20 d.

Functional analysis of *OsMOT1;1* in yeast

The molybdate transporting activity of OsMOT1;1 in yeast was determined according to previous studies with modifications [12]. To generate the plasmids for expression of *OsMOT1;1* in yeast (*Saccharomyces cerevisiae*), the full-length coding sequence of *OsMOT1;1* was PCR amplified from the cDNA of TQ or LM using the primers listed in Table S2. The correct PCR fragments confirmed by sequencing were subcloned into the *Eco*RI-*Xho*I site of the yeast expression vector pYX222x (Tomatsu *et al.*, 2007). The expression of *OsMOT1;1* in this plasmid was driven by a constitutive triose phosphate isomerase promoter. The resultant plasmids and empty vector were transformed into yeast strain BY4741 (MATa his3Δ1 leu2Δ0 met15Δ0 ura3Δ0) using a Frozen-EZ Yeast Transformation II Kit (ZYMO Research). For molybdate transporting assay, the BY4741 strains transformed with the empty vector pYX222x, *pYX222x-OsMOT1;1(TQ)* or *pYX222x-OsMOT1;1(LM)* were inoculated at 30°C overnight in 3 mL of Mo-free SD/-His media (6.7 g L^{-1} yeast nitrogen base without amino acids and without molybdenum (FORMEDIUM), 1.92 g L^{-1} dropout mix without histidine, 2% (w/v) glucose). A 100 µL sample of overnight yeast cells was then transferred to 10 ml Mo-free SD/-His media and incubated at 30°C until the optical density at 600 nm (O.D.600) reached to around 1.

Hexaammonium heptamolybdate was then added to the media to a final concentration of 0.5 μM. After shaking at 30°C for 30 min, yeast cells were harvested by centrifugation and then washed three times with 1mM EDTA-Na and once with Milli-Q water. Cells were dried at 80°C overnight, then digested with concentrated HNO_3. The Mo concentration in digested samples were determined by ICP-MS. The amount of yeast was converted by 1ml of 1 O.D.600 culture containing 3×10^7 cells (Baxter *et al.*, 2008).

To test the sulfate transporting activity of OsMOT1;1, the empty vector pYX222x, *pYX222x-OsMOT1;1(TQ)* and *pYX222x-OsMOT1;1(LM)* were transformed into a yeast mutant CP154-7B (MATa, his3, leu2, ura3, ade2, trp1, sul1::LEU2, sul2::URA3) as above (Tomatsu *et al.*, 2007). An *A. thaliana* high-affinity sulfate transporter gene *SULTR1;2* was used as positive control. The overnight yeast cultures were collected by centrifugation and washed once with Milli-Q water. After adjusting the O.D.600 of yeast cultures to 0.5, 10 μL yeast suspensions were spotted on synthetic medium (0.5 mM sulfate, 20 g L^{-1} glucose, 10 g L^{-1} agarose, 20 mg L^{-1} Ade, 30 mg L^{-1} L Leu, 20 mg L^{-1} Ura, and 20 mg of L^{-1} Trp) with or without 20 mg L^{-1} methionine. The plates were incubated at 30°C for 6 days.

Other methods could be found in Methods S1.

Results

Map-based cloning of *qGMo8*

We previously used two synthetic rice mapping populations composed of recombinant inbred lines derived from a cross between Lemont (LM, *japonica*) and TeQing (TQ, *indica*) (LT-RILs), and TeQing-into-Lemont backcross introgression lines (TILs), to identify QTLs that control the variation in concentration of 16 elements in unmilled rice grain (Zhang *et al.*, 2014). 134 QTLs were identified in either one or both mapping populations grown under flooded and/or unflooded field conditions (Zhang *et al.*, 2014). Among 8 QTLs that control the variation in grain Mo concentration, one was detected on the top of chromosome 8 (designated as *qGMo8*) in both mapping populations in field trials over multiple years and in both flooded and unflooded fields. This QTL explains up to 35% of

the variation in grain Mo (Fig. 1a and 1b). The *qGMo8* first observed in grain from field grown materials was also detected in both grain and leaf tissues from greenhouse grown TILs, which allows us to fine map the QTL using plants cultivated in the greenhouse (Fig. 1b).

To narrow down the *qGMo8* mapping interval, we developed additional markers to genotype the TIL population. Integration of grain Mo concentration and genotype data of three TILs narrowed the QTL interval down to a 522 kb region on the top of chromosome 8 (Fig. 1c). In this region, a gene (LOC_Os08g01120) annotated as sulfate transporter encodes a protein that shows 57.8% sequence similarity to *A. thaliana* high-affinity molybdate transporter AtMOT1;1 (Tomatsu *et al.*, 2007; Baxter *et al.*, 2008), which makes it a strong candidate gene for *qGMo8* (Fig. S1a). We thus designated LOC_Os08g01120 as *OsMOT1;1*. Sequence analysis revealed a 9-basepair (bp) deletion (Del^{9}) and a single nucleotide polymorphism (SNP) in the coding sequence of *OsMOT1;1* in TQ (Fig. 1d, Fig. S1b). The 9-bp deletion alters the amino acid sequence from four glutamines in LM to a glutamic acid in TQ (Fig. 1d, Fig. S1b). The SNP in the coding sequence also alters the amino acid sequence, with an alanine in LM and a serine in TQ at the position of 125 (S125A) (Fig. 1d, Fig. S1b). A 222-bp deletion (Del^{222}) and a 16-bp deletion (Del^{16}) were found in the promoter sequence of *OsMOT1;1* in TQ. Meanwhile, there are 19 SNPs in the promoter sequence of *OsMOT1;1* in TQ. Comparison of *OsMOT1;1* sequences of TQ and LM with Nipponbare reference sequence identified a 12-bp deletion (Del^{12}) in the coding region of *OsMOT1;1* in both TQ and LM, and only a SNP in the promoter sequence of *OsMOT1;1* between LM and Nipponbare (Fig. 1d). Sequence alignment showed that none of the variable amino acids between TQ and LM are conserved in the MOT1 protein family (Fig. S1a), suggesting that these amino acids might not alter the function of OsMOT1;1.

The existence of residual heterozygosity in TILs is useful for developing appropriate nearly isogenic lines (NIL) by generating heterogeneous inbred families (HIFs) (Tuinstra *et al.*, 1997; Loudet *et al.*, 2005; Huang *et al.*, 2016b). We identified TIL669.4 which is heterozygous at the *OsMOT1;1* locus, and isolated HIF669.4-TQ and HIF669.4-LM in the next generation (Fig. S2). These two HIFs have similar genomic background and only differ in a small genomic region containing homozygous *OsMOT1;1* alleles from TQ or LM, respectively. Both grain and leaf Mo concentrations of HIF669.4-TQ are significant

lower than that of HIF669.4-LM, suggesting that the TQ allele is a weak allele (Fig. 1e). Quantitative RT-PCR analysis showed that the expression levels of *OsMOT1;1* in both shoots and roots of HIF669.4-TQ were significantly lower than that of HIF669.4-LM, suggesting that the low Mo in HIF669.4-TQ might be due to the lower expression level of *OsMOT1;1* (Fig. 1f).

OsMOT1;1* is the causal gene for *qGMo8

To investigate the function of *OsMOT1;1*, we isolated a T-DNA insertion mutant of *OsMOT1;1*. The T-DNA insertion at the promoter of *OsMOT1;1* significantly decreases its expression (Fig. S3a- S3c). The *osmot1;1* mutant has no obvious phenotype difference from the wild-type (WT) when grown in soil in a greenhouse (Fig. 2a). Elemental profile analysis showed that the Mo concentration in the grain of *osmot1;1* is approximately 58% lower than that of the WT ($P < 0.001$, Student's *t*-test, $n = 10$) (Fig. 2b and 2c). The low Mo phenotype was also observed in the blades and sheaths of *osmot1;1* (Fig. 2b). Of the 22 elements determined, Mo is the only element that is significantly changed in the grain, leaves and sheaths of *osmot1;1*, suggesting a specific effect of *OsMOT1;1* mutation on Mo concentrations (Fig. 2c). To test whether *OsMOT1;1* is the causal gene for *qGMo8*, we performed an allelic complementation by crossing *osmot1;1* as well as WT with HIF669.4-TQ and HIF669.4-LM, respectively. The expression level of *OsMOT1;1* in the roots of both HIF669.4-TQ and HIF669.4-LM was higher than in that of *osmot1;1* (Fig. S3e). The Mo concentrations in both leaves and grain of *osmot1;1* × HIF669.4-TQ and *osmot1;1* × HIF669.4-LM F1 plants grown in soil in a greenhouse were significantly higher than that of *osmot1;1* (Fig. 2d and 2e), similar to the levels in HIF669.4-TQ and HIF669.4-LM, respectively, suggesting the complementation of *OsMOT1;1* from both TQ and LM to the knockout allele. However, significant differences of both leaf and grain Mo concentrations between *osmot1;1* × HIF669.4-TQ F1 and *osmot1;1* × HIF669.4-LM F1 were observed (Fig. 2d and 2e), indicating differential functional activity of OsMOT1;1 between TQ and LM. To further confirm *OsMOT1;1* as the causal gene, we crossed *osmot1;1* with *OsMOT1;1* overexpression lines in which *OsMOT1;1* from either TQ or LM was expressed from a cauliflower mosaic virus (CaMV) 35S promoter in the cv. Zhonghua 11 background. When grown in soil in a greenhouse, the Mo concentrations in grains of F2 plants containing the transgene in homozygous *osmot1;1* mutant background was significantly

higher than those homozygous *osmot1;1* plants without the transgene (Fig. 2e). These results demonstrate that overexpression of *OsMOT1;1* is able to complement the low Mo phenotype of the *osmot1;1* mutant.

Low Mo Phenotype of *osmot1;1* knockout mutant

At grain maturity stage, the *osmot1;1* mutant grown in soil in the greenhouse has a lower concentration of Mo than WT not only in the grain, but also in the blade and sheath of the flag leaf, and most of the nodes and internodes of the main tiller (Fig. 3a). Analysis of the seedlings grown hydroponically in the nutrient solution containing 1 nM Mo showed that *osmot1;1* accumulated significant lower Mo in both roots and shoots (Fig. 3b and 3c). However, the difference in the root Mo concentration between *osmot1;1* and WT disappeared when plants were grown in the nutrient solution containing 10 nM or higher concentration of Mo (Fig. 3b). Similarly, significant differences in the shoot Mo concentration were observed only at the low levels of Mo supply (1 and 10 nM), but not at the high levels of Mo supply (100 nm or 1 μM) (Fig. 3c). These results suggest that *OsMOT1;1* might function mainly at low Mo concentration. Consistent with lower Mo level in shoots, the Mo concentration in the xylem sap of *osmot1;1* was significantly decreased compared to the WT (Fig. 3d), suggesting that Mo translocation from roots to shoots was affected in *osmot1;1*. Further analysis showed that the Mo concentrations in all tissues except the leaf sheaths of the 5^{th} and 6^{th} leaves of *osmot1;1* were significantly lower than that of WT (Fig. 3e).

The *osmot1;1* mutant is sensitive to limited Mo supply

Given that *osmot1;1* accumulates less Mo in shoots, we investigated the sensitivity of *osmot1;1* to Mo deficiency. The bioavailability of Mo is strongly dependent on the soil pH with Mo becoming much less bioavailable in acid soils (Marschner & Rengel, 2012). When grown in acidified solid media without supplementation of Mo, most of the seeds of *osmot1;1* did not germinate, and the growth of the plants from seeds that did germinate was strongly inhibited (Fig. 4a and 4b). In contrast, the WT plants were able to germinate and grow, even though the root growth was also inhibited by low pH (Fig. 4a and 4b). These results establish that, without Mo added into the media, *osmot1;1* is more sensitive to low pH compared to the WT. Supplementation of 1 μM Mo to the acidified solid media

was able to restore the growth of *osmot1;1* to the level of WT (Fig. 4a and 4b), indicating that the sensitivity of *osmot1;1* to low pH is due to the deficiency of Mo in the media. We further showed that the HIF669.4-TQ, which accumulated less Mo (Fig. 1e), was more sensitive to Mo deficiency at low pH condition compared to the HIF669.4-LM (Fig. S4a and S4b).

Expression pattern and subcellular localization of OsMOT1;1

OsMOT1;1 was expressed in most of the plant tissues throughout the growth period of LM except the panicles at the reproductive stage (Fig. 5a). However, the expression of *OsMOT1;1* was much stronger in the roots than in the other tissues. In roots of 2-week-old seedlings, *OsMOT1;1* was strongly expressed in the lateral roots as investigated by *OsMOT1;1* promoter-GUS transgenic rice plants (Fig. 5b). Low levels of GUS signals were detected in other tissues. To test whether the expression of *OsMOT1;1* was affected by Mo supply, LM plants were grown in nutrient solution containing 1 μM Mo for one week and transferred to nutrient solution with Mo omitted for a further week. The expression of *OsMOT1;1* in roots was strongly suppressed by Mo depletion as determined by qRT-PCR. However, such suppression was not found in shoots (Fig. 5c).

To investigate the subcellular localization of OsMOT1;1, OsMOT1;1 from TQ or LM was fused with GFP to the C-terminal and expressed under the control of 35S promoter in a japonica variety Zhonghua 11 (Fig. S3d). The GFP fluorescence was co-localized with the signal of a mitochondrial dye Mitotacker, suggesting OsMOT1;1 localizes to the mitochondria (Fig. 5d). We observed that OsMOT1;1 from both TQ and LM were localized to the mitochondria, indicating that the amino acid variation of OsMOT1;1 between TQ and LM has no effect on the subcellular localization (Fig. 5d). Furthermore, the Mo concentrations in roots and shoots of transgenic lines were higher than the non-transgenic control line, suggesting the mitochondria-localized OsMOT1;1 is functional (Fig. S5).

Functional analysis of *OsMOT1;1* in *A. thaliana*

OsMOT1;1 shares 57.8% sequence similarity to AtMOT1;1 (Fig. S1a), a high-affinity molybdate transporter in *A. thaliana*. The *atmot1;1* mutant accumulates lower levels of Mo in leaves than WT (Tomatsu *et al.*, 2007; Baxter *et al.*, 2008). To investigate whether expression of *OsMOT1;1* in *atmot1;1* could suppress its low Mo phenotype, we

heterologously expressed *OsMOT1;1-GFP* in *atmot1;1* using 35S promoter (Fig. S6). In the root cells of the transgenic plants, the GFP signals were observed to co-localize with the mitochondria specific dye MitoTracker (Fig. S7), further confirming the mitochondria localization of OsMOT1;1. The Mo concentrations in both roots and shoots of transgenic plants expressing *OsMOT1;1* from either TQ or LM were significantly higher than that of *atmot1;1*, even higher than the WT Col-0 (Fig. 6a). These results suggest that expression of *OsMOT1;1* from either TQ or LM could enhance Mo accumulation in *atmot1;1*. To rule out the ectopic effect of overexpression of *OsMOT1;1* driven by 35S promoter, we also expressed *OsMOT1;1* in *atmot1;1* using *AtMOT1;1* native promoter (Fig. S6). The Mo concentrations in both roots and shoots of transgenic plants were significantly higher than that of *atmot1;1*, similar to the level in WT Col-0 (Fig. 6b), suggesting that expression of *OsMOT1;1* using *AtMOT1;1* native promoter was able to complement the *AtMOT1;1* knockout mutant. Notably, there was no significant difference in either root or shoot Mo concentration between transgenic plants expressing *OsMOT1;1* from TQ or LM (Fig. 6b), indicating no functional difference between the *OsMOT1;1* allele of TQ and LM. Previous studies have shown that the *atmot1;1* mutant is sensitive to low Mo stress (Tomatsu *et al.*, 2007) and shows defective growth in acidic soil in which the bioavailability of Mo is low (Poormohammad Kiani *et al.*, 2012). Similar to the sensitivity to acidic soil, *atmot1;1* also showed growth inhibition on agar media at low pH without added Mo (Fig. 6c to 6e). The transgenic plants expressing *OsMOT1;1* from TQ or LM using 35S promoter or *MOT1* native promoter completely restore the growth of *atmot1;1* on agar media at low pH (Fig. 6c to 6e). The results further confirm that *OsMOT1;1* is able to complement the mutation of *AtMOT1;1* in *A. thaliana*.

Molybdate transport activity of OsMOT1;1

The molybdate transport activity of OsMOT1;1 was tested by heterologous expression of *OsMOT1*;1 in yeast (*Saccharomyces cerevisiae*) strain BY4741. Yeast strain BY4741 transformed with empty vector or *OsMOT1;1* from TQ or LM were cultured in Mo-free media to the mid-log phase and then transferred to the media containing 0.5 µM Mo and incubated for 30 min. The Mo concentration in yeast cells transformed with *OsMOT1;1* was significantly higher than the control strain transformed with an empty vector (Fig. 7a). These results support the conclusion that OsMOT1;1 is able to transport molybdate. Further

comparison revealed no difference of Mo concentrations in the strains transformed with *OsMOT1;1* from TQ or LM (Fig. 7a), indicating that OsMOT1;1 from TQ and LM exhibited similar molybdate transporting activity.

OsMOT1;1 shares sequence similarity to sulfate transporter genes in rice and thus was previously annotated as a member of the group five sulfate transporter family (Kumar *et al.*, 2011). To determine whether OsMOT1;1 exhibits a sulfate transport activity, we performed complementation analysis of a yeast mutant CP154-7B, which is defective in two high-affinity sulfate transporters and is unable to grow on the media containing lower than 1 mM sulfate as the sole sulfur source (Shibagaki *et al.*, 2002; Yoshimoto *et al.*, 2002; Tomatsu *et al.*, 2007). The yeast mutant transformed with *SULTR1;2*, an *A. thaliana* high-affinity sulfate transporter, was able to grow on the – Met media. However, expression of *OsMOT1;1* from either TQ or LM was unable to complement the growth defect of the mutant strain on –Met media (Fig. 7b). These results suggest that OsMOT1;1 likely does not exhibit sulfate transport activity.

Analysis of natural variation of *OsMOT1;1*

To investigate the contribution of natural variation at *OsMOT1;1* to the variation of grain Mo in rice, we analyzed the coding sequences of 1,479 rice accessions which have been resequenced (Zhao *et al.*, 2015). Five non-synonymous polymorphisms in the coding sequence of *OsMOT1;1* were identified, including the two polymorphic sites between TQ and LM (S125A and Del^{9}), and the 12 bp deletion (Del^{12}) in both TQ and LM (Table S1 and Fig. 1d). To determine the contribution of these three polymorphic sites on the variation of grain Mo, we genotyped 1,097 accessions of USDA rice core collection for which we have previously reported the grain ionomic profile (Pinson *et al.*, 2015). We found no significant difference of grain Mo between the two alleles on any of these three polymorphic sites (Fig. 8a, Fig. S8a). We further compared the grain Mo concentrations of eight haplotypes derived from the combination of these three polymorphic sites. We observed no significant differences of grain Mo among the eight haplotypes (Fig. 8b and Fig. S8b). These results suggested that the variation in the coding region of *OsMOT1;1* might not contribute to the variation of grain Mo in the rice population.

There are 19 SNPs and two sequence deletions (Del^{222} and Del^{16}) in the promoter sequence of *OsMOT1;1* in TQ (Fig. 1d). We determined the contribution of the two major sequence variances, Del^{222} and Del^{16}, on the variation of grain Mo. We genotyped the 1,097 accessions of USDA core collection and compared the grain Mo concentrations of accessions with or without the deletions. We found that there was no significant difference between the accessions with or without the Del^{222} or Del^{16} (Fig. 8c and Fig. S8c). Furthermore, the grain Mo concentrations among the accessions with combination of Del^{222} and Del^{16} were fairly similar (Fig. 8d and Fig. S8d). These results suggested that Del^{222} and Del^{16} in the promoter of *OsMOT1;1* might not contribute to the variation of grain Mo. Thus, the different promoter activity of *OsMOT1;1* between TQ and LM was likely due to the 19 SNPs, which might cause different expression level of *OsMOT1;1* between TQ and LM.

Correlation of grain Mo with the expression of *OsMOT1;1*

To determine whether the variation of grain Mo was due to the variation in the *OsMOT1;1* expression level, we selected 35 rice accessions from the USDA core collection with grain Mo concentrations ranging from 0.063 to 1.52 μg g^{-1} under flooded growth condition and 0.084 to 1.23 μg g^{-1} under unflooded condition. The expression levels of *OsMOT1;1* were determined in the roots of three-week-old plants grown hydroponically with 1 μM Mo. We found highly significant correlations between the expression level of *OsMOT1;1* in roots from hydroponically grown plants with the Mo concentrations in grains from plants grown in the field under both flooded (Pearson's $R^2 = 0.7368$, $p < 0.001$) (Fig. 8e) and unflooded (Pearson's $R^2 = 0.6207$, $p < 0.001$) conditions (Fig. S8e). These results suggest the natural variation of Mo concentration in rice grains is attributed to the variable expression of *OsMOT1;1* in roots.

Discussion

As one of the essential mineral nutrients required by plants, Mo plays important roles in nitrate assimilation, abscisic acid biosynthesis, purine degradation and sulfite detoxification (Schwarz & Mendel, 2006; Bittner, 2014). However, the mechanisms of Mo uptake and transport and the regulation these processes are largely unknown in plants,

especially in crops. In this study, we identified a QTL *qGMo8* that controls the variation of Mo concentration in rice shoots and grains. We determined the causal gene for this QTL to be *OsMOT1;1* by genetic and transgenic complementation (Fig. 2d and 2e). OsMOT1;1 was previously annotated as a member of the group V sulfate transporter superfamily (Tejada-Jimenez *et al.*, 2013). We provided evidence that OsMOT1;1 is a molybdate transporter, including the fact that OsMOT1;1 enhances molybdate but not sulfate uptake when heterogeneously expressed in yeast (Fig. 7a and 2b). We found that the difference in grain Mo concentrations between rice cultivars TQ and LM was not due to altered molybdate transporting activity but most likely to the allelic variation at the gene expression level of *OsMOT1;1*. This conclusion is supported by several lines of evidence. First, the molybdate transporting activity of OsMOT1;1 from TQ and LM was similar when heterogeneously expressed in yeast (Fig. 7a). Second, the *OsMOT1;1* from either TQ or LM was able to complement the low Mo phenotype of *atmot1;1* to a similar level when expressed by the *AtMOT1;1* native promoter (Fig. 6b, 6c and 6e). Third, the heterogeneous inbred families line HIF669.4-LM with higher expression level of *OsMOT1;1* accumulates more Mo in the leaves and grains than that of HIF669.4-TQ. Knockout of *OsMOT1;1* resulted in decreased Mo concentration in the shoots and grains (Fig. 2b and 2c). We thus conclude that OsMOT1;1 is a molybdate transporter in rice and the natural variation of Mo concentration in rice grains is attributed to the allelic variation at the gene expression level of *OsMOT1;1*.

Several molybdate transporters have been identified, including CrMOT1 and CrMOT2 from *C. reinhardtii* (Tejada-Jimenez *et al.*, 2007; Tejada-Jimenez *et al.*, 2011), AtMOT1;1 and AtMOT1;2 from *A. thaliana* (Tomatsu *et al.*, 2007; Baxter *et al.*, 2008; Gasber *et al.*, 2011), LjMOT1 from *Lotus japonicus* (Gao *et al.*, 2016; Duan *et al.*, 2017) and MtMOT1.3 from *Medicago truncatula* (Tejada-Jimenez *et al.*, 2017). *AtMOT1;1* has been shown to control the natural variation in leaf Mo concentration in *A. thaliana* (Baxter *et al.*, 2008). A 53-bp deletion in the promoter of *AtMOT1;1* which is located 13 bp upstream from the transcription start-site of *AtMOT1;1* was identified as the functional polymorphism contributing to decreased leaf Mo concentration (Tomatsu *et al.*, 2007; Baxter *et al.*, 2008). Further analysis revealed a total of six non-coding structural polymorphisms in the *AtMOT1;1* promoter, including the 53-bp deletion originally identified in L*er*-0 and a

duplicated 330-bp insertion that has undergone a 4-bp deletion (Forsberg *et al.*, 2015). The 53-bp deletion is associated with decreased leaf Mo, while the duplicated 330-bp insertion is associated with elevated leaf Mo. These two polymorphisms control Mo concentration in leaves by either decreasing or increasing, respectively, the expression level of *AtMOT1;1*.

In this study, we identified 19 SNPs and two deletions, a 222-bp deletion (Del^{222}) and a 16-bp deletion (Del^{16}), in the promoter of *OsMOT1;1* between TQ and LM (Fig. 1d). We showed that the difference in grain Mo concentration between TQ and LM was due to the different expression level of *OsMOT1;1* (Fig. 1e and 1f). Further analysis of 35 rice accessions revealed a significant positive correlation between the expression level of *OsMOT1;1* in roots and Mo concentration in grains (Fig. 8e and Fig. S8e). However, the variation in grain Mo appears unrelated to the two main non-coding structural polymorphisms, Del^{222} and Del^{16}, as grain Mo concentrations of rice accessions with or without these two deletions were similar (Fig. 8c and 8d, Fig. S8c and S8d). Therefore, the difference in grain Mo concentration between TQ and LM may be due to the SNPs in the promoter of *OsMOT1;1* which lead to different expression level. At least two SNPs which are significantly associated with the variation of leaf Mo were also identified on the *AtMOT1;1* locus, even though the effect of these SNPs on its expression is not clear (Forsberg *et al.*, 2015). Thus, the variation of Mo in both rice and *A. thaliana* is attributed to the variable expression of the *MOT1;1* gene. Such conserved genetic variation structure across plant species suggests a role of *MOT1;1* gene in the adaptation to the environment. Indeed, *A. thaliana* accessions with the weak allele of *AtMOT1;1* from West Asia appear to adapt to their native habitats where the water extractable Mo content is high in soils (Poormohammad Kiani *et al.*, 2012). We found that the *osmot1;1* mutant is sensitive to limited Mo supply condition (Fig. 4a and 4b), similar to the sensitivity of *atmot1;1* to Mo deficiency (Tomatsu *et al.*, 2007) and to acidic soils in which the bioavailability of Mo is low (Poormohammad Kiani *et al.*, 2012). Therefore, the *MOT1;1* gene may play an important role in adaptation to variable molybdate availability in soils caused by environmental changes.

The polymorphisms in the coding region of *AtMOT1;1* also affect its function. A single amino acid variation on AtMOT1;1 in L*er*-0 accession alters its molybdate transporting activity (Tomatsu *et al.*, 2007). The hypofunction of AtMOT1;1 in Sha accession was also

proved to be caused by a single amino acid change (Poormohammad Kiani *et al.*, 2012). In the present study, we found two amino acid polymorphisms in OsMOT1;1 between TQ and LM (Fig. 1d). However, none of them appears to alter the function of OsMOT1;1 as these two version proteins showed similar molybdate transporting activity and was able to complement the low Mo phenotype of the *atmot1;1* mutant to a similar level (Fig. 6b, 6c and 6e; Fig. 7a). A 12-bp deletion (Del^{12}) in the coding region of *OsMOT1;1* of both TQ and LM, compared with Nipponbare, seems not to change its function because the presence/absence of Del^{12} is not associated with the variation of grain Mo (Fig. 8a and 8b, Fig. S8a and S8b). Thus, the large sequence diversity of the *MOT1;1* locus explains well the identification of *AtMOT1;1* in controlling the variation of leaf Mo by genome-wide association (GWA) analysis based on either the mean or variance of leaf Mo (Shen *et al.*, 2012; Forsberg *et al.*, 2015), and *OsMOT1;1* as the potential locus responsible for the variation of rice grain Mo concentration (Norton *et al.*, 2014).

The expression of *OsMOT1;1* is stronger in roots than in shoots (Fig. 5a), similar to the expression pattern of *AtMOT1;1* in *A. thaliana* (Tomatsu *et al.*, 2007), which is consistent with the fact that *AtMOT1;1* mainly functions in roots (Baxter *et al.*, 2008). Under Mo limited condition, *OsMOT1;1* is downregulated in roots but not in shoots (Fig. 5a). However, such downregulation was not observed for *AtMOT1;1* in roots but rather in shoots (Tomatsu *et al.*, 2007), suggesting the different behaviour of *MOT1;1* genes in rice and *A. thaliana* under Mo scarce condition. *OsMOT1;1* may mainly function under low Mo condition, as we only observed the difference of Mo concentrations between WT and *osmot1;1* in the hydroponic growth system containing 1 or 10 nM Mo but not at relative higher Mo condition (100 nM or 1 μM) (Fig. 3b and 3c). The Mo concentration in the xylem sap of *osmot1;1* is lower than that of WT (Fig. 3d), suggestion *OsMOT1;1* is also involved in the translocation of Mo from roots to shoots. Meanwhile, the Mo concentrations in the grain, blade and sheath of *osmot1;1* only decrease by 58% - 82% compared to the WT (Fig. 2d), suggesting the existence of additional transporters that control the accumulation of Mo in rice. Further studies are required to elucidate the detailed function of *OsMOT1;1* and to identify other transporters in controlling the Mo homeostasis in rice.

In summary, we have identified *OsMOT1;1* as the causal gene underlying the QTL for Mo accumulation in rice shoots and grains. OsMOT1;1 exhibits molybdate transport activity. The identification of *OsMOT1;1* provides an important insight into the regulation of Mo homeostasis in rice and a useful gene to breed rice varieties resistant to Mo deficiency in soils. Given the importance of cereals as a source of Mo in the human diet, the identification of natural variation at the *OsMOT1;1* locus provides an efficient way to breed rice varieties with Mo enrichment in the grain, which could improve the nutrient quality of grains.

Acknowledgments

We thank B. Lahner, E. Yakubova and John Danku for ICP-MS analysis, Long-Gang Cui and Min Shi for rice transformation, Takehiro Kamiya and Toru Fujiwara for providing pYX222x and pYX222x-SULTR1;2 vectors. We also thank the Rice Mutant Database at Huazhong Agricultural University for providing the T-DNA insertion line. This research was supported by the US National Science Foundation, Plant Genome Research Program (Grant #IOS 0701119 to D.E.S, M.L.G and S.R.M.P.), the Fundamental Research Funds for the Central Universities (KYZ201714 to X.-Y.H), the Natural Science Foundation of China (31520103914 to F.-J.Z. and D.E.S.; 31772382 to X.-Y.H) and Jiangsu Natural Science Foundation for Distinguished Young Scholars (KB20180023 to X.-Y.H).

Author contribution

X.-Y.H. and D.E.S. designed the research; X.-Y.H., H.L., Y.-F.Z., S.R.M.P., H.-X.L., and M.L.G. performed the experiments. X.-Y.H. and D.E.S. analysed the data. X.-Y.H., F.-J.Z., and D.E.S. wrote the paper with contributions of S.R.M.P. and M.L.G.

References

Arnon DI, Stout PR. 1939. Molybdenum as an essential element for higher plants. *Plant Physiology* **14**: 599-602.

Baxter I, Muthukumar B, Park HC, Buchner P, Lahner B, Danku J, Zhao K, Lee J, Hawkesford MJ, Guerinot ML, Salt DE. 2008. Variation in molybdenum content across broadly distributed populations of *Arabidopsis thaliana* is controlled by a mitochondrial molybdenum transporter (MOT1). *PLoS Genetics* **4**: e1000004.

Bittner F. 2014. Molybdenum metabolism in plants and crosstalk to iron. *Front Plant Sci* **5**: 28.

Clough SJ, Bent AF. 1998. Floral dip: a simplified method for Agrobacterium-mediated transformation of *Arabidopsis thaliana*. *Plant Journal* **16**: 735-743.

Duan G, Hakoyama T, Kamiya T, Miwa H, Lombardo F, Sato S, Tabata S, Chen Z, Watanabe T, Shinano T, Fujiwara T. 2017. LjMOT1, a high-affinity molybdate transporter from *Lotus japonicus*, is essential for molybdate uptake, but not for the delivery to nodules. *Plant Journal* **90**: 1108-1119.

Forsberg SK, Andreatta ME, Huang XY, Danku J, Salt DE, Carlborg O. 2015. The multi-allelic genetic architecture of a variance-heterogeneity locus for molybdenum concentration in leaves acts as a source of unexplained additive genetic variance. *PLoS Genetics* **11**: e1005648.

Gao JS, Wu FF, Shen ZL, Meng Y, Cai YP, Lin Y. 2016. A putative molybdate transporter LjMOT1 is required for molybdenum transport in *Lotus japonicus*. *Physiologia Plantarum* **158**: 331-340.

Gasber A, Klaumann S, Trentmann O, Trampczynska A, Clemens S, Schneider S, Sauer N, Feifer I, Bittner F, Mendel RR, Neuhaus HE. 2011. Identification of an Arabidopsis solute carrier critical for intracellular transport and inter-organ allocation of molybdate. *Plant Biology (Stuttgart, Germany)* **13**: 710-718.

Grunden AM, Shanmugam KT. 1997. Molybdate transport and regulation in bacteria. *Archives of Microbiology* **168**: 345-354.

Hiei Y, Ohta S, Komari T, Kumashiro T. 1994. Efficient transformation of rice (*Oryza sativa* L.) mediated by Agrobacterium and sequence analysis of the boundaries of the T-DNA. *Plant Journal* **6**: 271-282.

Hollenstein K, Frei DC, Locher KP. 2007. Structure of an ABC transporter in complex with its binding protein. *Nature* **446**: 213-216.

Huang XY, Chao DY, Gao JP, Zhu MZ, Shi M, Lin HX. 2009. A previously unknown zinc finger protein, DST, regulates drought and salt tolerance in rice via stomatal aperture control. *Genes & Development* **23**: 1805-1817.

Huang XY, Chao DY, Koprivova A, Danku J, Wirtz M, Muller S, Sandoval FJ, Bauwe H, Roje S, Dilkes B, Hell R, Kopriva S, Salt DE. 2016a. Nuclear localised MORE

SULPHUR ACCUMULATION1 epigenetically regulates sulphur homeostasis in Arabidopsis thaliana. *PLoS Genetics* **12**: e1006298.

Huang XY, Deng F, Yamaji N, Pinson SR, Fujii-Kashino M, Danku J, Douglas A, Guerinot ML, Salt DE, Ma JF. 2016b. A heavy metal P-type ATPase OsHMA4 prevents copper accumulation in rice grain. *Nature Communications* **7**: 12138.

Johnson JL, Waud WR, Rajagopalan KV, Duran M, Beemer FA, Wadman SK. 1980. Inborn errors of molybdenum metabolism: combined deficiencies of sulfite oxidase and xanthine dehydrogenase in a patient lacking the molybdenum cofactor. *Proceedings of the National Academy of Sciences of the United States of America* **77**: 3715-3719.

Kaiser BN, Gridley KL, Ngaire Brady J, Phillips T, Tyerman SD. 2005. The role of molybdenum in agricultural plant production. *Annals of Botany* **96**: 745-754.

Kumar S, Asif MH, Chakrabarty D, Tripathi RD, Trivedi PK. 2011. Differential expression and alternative splicing of rice sulphate transporter family members regulate sulphur status during plant growth, development and stress conditions. *Functional and Integrative Genomics* **11**: 259-273.

Loudet O, Gaudon V, Trubuil A, Daniel-Vedele F. 2005. Quantitative trait loci controlling root growth and architecture in *Arabidopsis thaliana* confirmed by heterogeneous inbred family. *Theoretical and Applied Genetics* **110**: 742-753.

Marschner P, Rengel Z 2012. Nutrient availability in soils. *Mineral Nutrition of Higher Plants (Third Edition)*. San Diego: Academic Press, 315-330.

Norton GJ, Douglas A, Lahner B, Yakubova E, Guerinot ML, Pinson SR, Tarpley L, Eizenga GC, McGrath SP, Zhao FJ, Islam MR, Islam S, Duan G, Zhu Y, Salt DE, Meharg AA, Price AH. 2014. Genome wide association mapping of grain arsenic, copper, molybdenum and zinc in rice (*Oryza sativa* L.) grown at four international field sites. *PloS One* **9**: e89685.

Pinson SRM, Liu GJ, Jia MH, Jia YL, Fjellstrom RG, Sharma A, Wang YG, Tabien RE, Li ZK. 2012. Registration of a rice gene-mapping population consisting of 'TeQing'-into-'Lemont' backcross introgression lines. *Journal of Plant Registrations* **6**: 128-135.

Pinson SRM, Tarpley L, Yan WG, Yeater K, Lahner B, Yakubova E, Huang XY, Zhang M, Guerinot ML, Salt DE. 2015. Worldwide genetic diversity for mineral element concentrations in rice grain. *Crop Science* **55**: 294-311.

Poormohammad Kiani S, Trontin C, Andreatta M, Simon M, Robert T, Salt DE, Loudet O. 2012. Allelic heterogeneity and trade-off shape natural variation for response to soil micronutrient. *PLoS Genetics* **8**: e1002814.

Schwarz G. 2005. Molybdenum cofactor biosynthesis and deficiency. *Cellular and Molecular Life Sciences* **62**: 2792-2810.

Schwarz G, Mendel RR. 2006. Molybdenum cofactor biosynthesis and molybdenum enzymes. *Annual Review of Plant Biology* **57**: 623-647.

Shen X, Pettersson M, Ronnegard L, Carlborg O. 2012. Inheritance beyond plain heritability: variance-controlling genes in *Arabidopsis thaliana*. *PLoS Genetics* **8**: e1002839.

Shibagaki N, Rose A, McDermott JP, Fujiwara T, Hayashi H, Yoneyama T, Davies JP. 2002. Selenate-resistant mutants of Arabidopsis thaliana identify Sultr1;2, a sulfate transporter required for efficient transport of sulfate into roots. *Plant Journal* **29**: 475-486.

Tabien RE, Li Z, Paterson AH, Marchetti MA, Stansel JW, Pinson SRM. 2000. Mapping of four major rice blast resistance genes from 'Lemont' and 'Teqing' and evaluation of their combinatorial effect for field resistance. *Theoretical and Applied Genetics* **101**: 1215-1225.

Tejada-Jimenez M, Chamizo-Ampudia A, Galvan A, Fernandez E, Llamas A. 2013. Molybdenum metabolism in plants. *Metallomics* **5**: 1191-1203.

Tejada-Jimenez M, Galvan A, Fernandez E. 2011. Algae and humans share a molybdate transporter. *Proceedings of the National Academy of Sciences of the United States of America* **108**: 6420-6425.

Tejada-Jimenez M, Gil-Diez P, Leon-Mediavilla J, Wen J, Mysore KS, Imperial J, Gonzalez-Guerrero M. 2017. Medicago truncatula Molybdate Transporter type 1 (MtMOT1.3) is a plasma membrane molybdenum transporter required for nitrogenase activity in root nodules under molybdenum deficiency. *New Phytologist* **216**: 1223-1235.

Tejada-Jimenez M, Llamas A, Sanz-Luque E, Galvan A, Fernandez E. 2007. A high-affinity molybdate transporter in eukaryotes. *Proceedings of the National Academy of Sciences of the United States of America* **104**: 20126-20130.

Tomatsu H, Takano J, Takahashi H, Watanabe-Takahashi A, Shibagaki N, Fujiwara T. 2007. An *Arabidopsis thaliana* high-affinity molybdate transporter required for efficient uptake of molybdate from soil. *Proceedings of the National Academy of Sciences of the United States of America* **104**: 18807-18812.

Tuinstra MR, Ejeta G, Goldsbrough PB. 1997. Heterogeneous inbred family (HIF) analysis: a method for developing near-isogenic lines that differ at quantitative trait loci. *Theoretical and Applied Genetics* **95**: 1005-1011.

von Uexküll HR, Mutert E. 1995. Global extent, development and economic impact of acid soils. *Plant and Soil* **171**: 1-15.

Yoshimoto N, Takahashi H, Smith FW, Yamaya T, Saito K. 2002. Two distinct high-affinity sulfate transporters with different inducibilities mediate uptake of sulfate in Arabidopsis roots. *Plant Journal* **29**: 465-473.

Zhang M, Pinson SR, Tarpley L, Huang XY, Lahner B, Yakubova E, Baxter I, Guerinot ML, Salt DE. 2014. Mapping and validation of quantitative trait loci associated with concentrations of 16 elements in unmilled rice grain. *Theoretical and Applied Genetics* **127**: 137-165.

Zhao H, Yao W, Ouyang Y, Yang W, Wang G, Lian X, Xing Y, Chen L, Xie W. 2015. RiceVarMap: a comprehensive database of rice genomic variations. *Nucleic Acids Research* **43**: D1018-1022.

Figure legends

Fig. 1. QTL analysis and cloning of *qGMo8*.

(a and b) The LOD profiling of *qGMo8* on chromosome 8 in the LT-RIL population (a) and TIL population (b) grown in multiple years under different conditions. F, flooded; U, unflooded. G, grains of TILs grown in greenhouse; L, leaves of greenhouse grown TILs. (c) Grain Mo concentration and genotype at QTL interval of selected TILs. Data are presented as mean ± SD (n = 3). Columns with different letters indicate significant difference at $P \leq 0.01$ (Tukey's Honestly Significant Difference (HSD) test). DW, dry weight. (d) Gene structure and sequence variation of *OsMOT1;1* among Nipponbare (Nipp), TQ and LM. Blue bars and white bars represent exons and untranslated regions, respectively. Vertical lines represent SNPs. (e) The Mo concentration in the grain and leaf of HIF669.4-TQ and HIF669.4-LM. (f) Expression level of *OsMOT1;1* in shoots and roots of HIF669.4-TQ and HIF669.4-LM. Data in (e) and (f) are presented as mean ± SD with n = 6 in (e) and 3 in (f). ** indicates significant difference at $P \leq 0.01$ (Student's t test).

Fig. 2. Characterization of the *osmot1;1* mutant and complementation test.

(a) Greenhouse grown WT and *osmot1;1* plants grown at harvesting stage. (b) Mo concentrations in the grain, blade and sheath of WT and *osmot1;1*. Data are presented as means ± SD (n = 8). ** indicates significant difference between WT and *osmot1;1* at $P \leq$

0.01 (Student's *t* test). (c) Percentage difference of 22 elements in the grain, blade and sheath of *osmot1;1* compared with the WT. Data are visualized in the radar chart. (d) Genetic complementation of *osmot1;1* by crossing with HIF669.4-TQ or HIF669.4-LM. The Mo concentrations in the grain of F1 plants were determined. (e) Transgenic complementation of *osmot1;1* by crossing with *OsMOT1;1* overexpression lines. The grain Mo concentrations of F2 plants in a homozygous mutant background containing *35S:OsMOT1;1(TQ)-GFP* or *35S:OsMOT1;1(LM)-GFP* constructs were determined. Two independent complemented lines were used for crossing. Data in (d, e) are presented as boxplots (n = 6). Boxes with different letters indicate significant difference at $P \leq 0.01$ (Tukey's HSD test). DW, dry weight.

Fig. 3. **Low Mo phenotype of the *osmot1;1* mutant.**

(a) The Mo concentrations in different tissues of greenhouse grown WT and *osmot1;1* plants at harvesting stage. (b and c) The Mo concentrations in roots (b) and shoots (c) of WT and *osmot1;1*. Plants were hydroponically grown in nutrient solution containing various concentrations of Mo for two weeks. (d) The Mo concentration in the xylem sap of WT and *osmot1;1*. Plants were hydroponically grown in Mo-free nutrient solution for one week and treated with various concentrations of Mo for another week. (e) The Mo concentrations in different tissues of WT and *osmot1;1* seedlings. Plants were hydroponically grown in nutrient solution containing 10 nM of Mo for two weeks. Data (a) are presented as boxplots (n = 11 for WT and n = 10 for *osmot1;1*). Data in (b-e) are presented as means ± SD with n = 4 in (b, c), 8 in (d, e). * and ** indicate significant difference between WT and *osmot1;1* at $P \leq 0.05$ and 0.01 (Student's *t* test), respectively. DW, dry weight.

Fig. 4. The *osmot1;1* mutant is sensitive to Mo deficiency at low pH condition.

(a) The phenotype of WT and *osmot1;1* grown under normal or low pH media with or without 1 μM Mo added. Low pH media was made by adding 50 μL 6 M HCl to 100 mL agar media after autoclaving. Plants were grown for 20 days. Bar, 3 cm. (b) The plant height of WT and *osmot1;1* grown as in (a). Data are presented as means ± SD with n = 6. *** indicated significant difference between WT and *osmot1;1* at $P \leq 0.001$ (Student's *t* test).

Fig. 5. **Expression pattern of *OsMOT1;1***.

(a) Expression level of *OsMOT1;1* in different organs of Lemont at different growth stages. (b) Histochemical GUS staining of roots of transgenic rice plants transformed with *OsMOT1;1* promoter driven GUS constructs. The mature zone (left), elongation zone (middle) and root tip (right) of roots of 2-week-old plants are showed. Scale bars from left to right are 2, 0.5 and 2 mm. (c) Expression of *OsMOT1;1* was suppressed in roots under Mo deficiency. Lemont (LM) plants were grown hydroponically with 1 μM Mo for one week and then treated with 1 μM Mo (+Mo) or without Mo (-Mo) for another week. Relative expression level of was determined by qRT-PCR with three biological replicates. ** indicates significant difference at $P \leq 0.01$ (Student's *t* test). (d) Subcellular localization of OsMOT1;1 in stable transgenic rice plants. OsMOT1;1 from TeQing (TQ) or LM were fused with GFP at N-terminal and overexpressed under the control of CaMV 35S promoter. Mitochondria were stained with the specific dye MitoTracker. Scale bar, 10 μm.

Fig. 6. **Functional analysis of *OsMOT1;1* in *Arabidopsis atmot1;1* mutant.**

(a and b) Mo concentrations in roots and shoots of the *mot1* mutant transformed with *OsMOT1;1-GFP* from TeQing (TQ) or Lemont (LM) driven by CaMV 35S promoter (a) or *AtMOT1;1* native promoter (b). Plants were grown on MGRL media containing 24 nM Mo for two weeks. Three independent transgenic lines are shown. (c) Phenotype of *OsMOT1;1-GFP* transgenic lines in *mot1* background. Plants were grown on MGRL media without added Mo at control or low pH condition for 20 days. Bar, 1 cm. (d and e) Fresh weight of *mot1* transformed with *OsMOT1;1-GFP* from TeQing (TQ) or Lemont (LM) driven by CaMV 35S promoter (d) or *AtMOT1;1* native promoter (e). Plants were grown as in (c). Three independent transgenic lines are shown. Data in (a) and (b) are shown as means ± SD with three biological replicates. Six plants were combined in each replicate. Data in (d) and (e) are shown as boxplots with $n = 7$ to 12. Columns or boxplots with different letters in (a) to (e) indicate significant difference at $P \leq 0.01$ (Tukey's HSD test). DW, dry weight.

Fig. 7. **Functional analysis of *OsMOT1;1* in yeast.**

(a) Molybdate transport activity of OsMOT1;1. Yeast strains transformed with empty vector, or *OsMOT1;1* from TeQing (TQ) or Lemont (LM) were incubated in media

containing 0.5 μM Mo for 30 min. Mo concentrations in yeast cells were determined. Data are shown as boxplot with n = 3. Boxplots with different letters indicate significant difference at $P \leq 0.01$ (Tukey's HSD test). (b) Complementation analysis of a yeast mutant defective in sulfate uptake. The yeast mutant strains transformed with empty vector, *SULTR1;2*, or *OsMOT1;1* from TQ or LM were incubated on media containing 0.5 mM sulfate with or without added Met for four days.

Fig. 8. **Contribution of allelic variation of *OsMOT1;1* on the variation of grain Mo in USDA rice core collection grown in flooded condition.**

(a) The grain Mo in rice accessions with different alleles at three polymorphic sites in the coding region of *OsMOT1;1*. (b) The grain Mo in rice accessions with different haplotypes derived from the combination of three polymorphic sites in the coding region of *OsMOT1;1*. (c) The grain Mo in rice accessions with or without the deletions in the promoter region of *OsMOT1;1*. (d) The grain Mo in rice accessions with different promoter haplotypes derived from the combination of two deletions in the coding region of *OsMOT1;1*. Data in (a - d) are shown as boxplots. Numbers under the boxes are the accession number; numbers above the boxes are the *P* values; the same letters above the boxes indicate no significant difference at $P \leq 0.01$ (Tukey's HSD test). + and – represent the presence and absence of the deletion, respectively. The dash color boxes in (b) and (d) mark the haplotypes in TQ , LM and Nipp. (e) The correlation of the relative expression of *OsMOT1;1* in roots with the grain Mo concentration in 35 rice accessions grown in flooded condition. The expression of *OsMOT1;1* in the roots of 3-week-old plants were determined by qRT-PCR. The relative expression level of *OsMOT1;1* was normalized the rice actin gene, and presented as the mean of 2^(-deltaCt) with three biological replicates.

Supporting Information

Additional supporting information may be found in the online version of this article.

Fig. S1 Sequence alignment of MOT1 proteins.

Fig. S2 Schematic diagram of development of heterogeneous inbred families (HIF).

Fig. S3 Molecular characterization of OsMOT1;1 T-DNA insertion and OsMOT1;1 overexpression lines.

Fig. S4 The sensitivity of HIF669.4-TQ and HIF669.4-LM to Mo deficiency at low pH condition.

Fig. S5 Overexpression of *OsMOT1;1* increases Mo concentrations in both roots and shoots.

Fig. S6 Expression level of OsMOT1;1 in Arabidopsis transgenic lines.

Fig. S7 Subcellular localization of OsMOT1;1 in Arabidopsis.

Fig. S8 Contribution of allelic variation of OsMOT1;1 on the variation of grain Mo in USDA rice core collection grown in unflooded condition.

Table S1. Sequence variation and allele frequency of OsMOT1;1.

Table S2. The primers used in this study.

Methods S1 Supporting information for Materials and Methods.

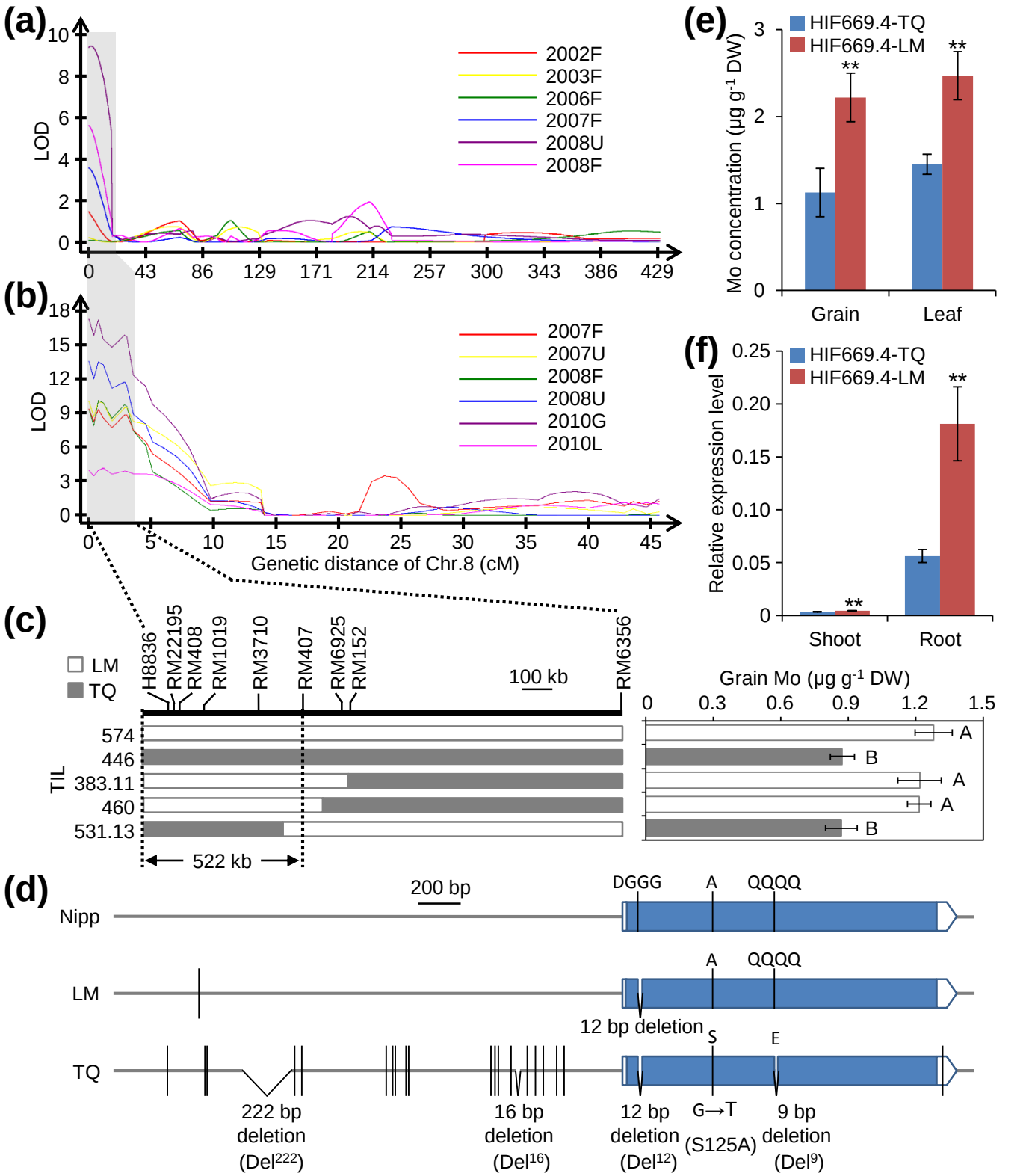

Fig 1. **QTL analysis and cloning of *qGMo8*.**
(a and b) The LOD profiling of *qGMo8* on chromosome 8 in the LT-RIL population (a) and TIL population (b) grown in multiple years under different conditions. F, flooded; U, unflooded. G, grains of TILs grown in greenhouse; L, leaves of greenhouse grown TILs. (c) Grain Mo concentration and genotype at QTL interval of selected TILs. Data are presented as mean ± SD (n = 3). Columns with different letters indicate significant difference at $P \leq 0.01$ (Tukey's Honestly Significant Difference (HSD) test). DW, dry weight. (d) Gene structure and sequence variation of *OsMOT1;1* among Nipponbare (Nipp), TQ and LM. Blue bars and white bars represent exons and untranslated regions, respectively. Vertical lines represent SNPs. (e) The Mo concentration in the grain and leaf of HIF669.4-TQ and HIF669.4-LM. (f) Expression level of *OsMOT1;1* in shoots and roots of HIF669.4-TQ and HIF669.4-LM. Data in (E) and (f) are presented as mean ± SD with n = 6 in (e) and 3 in (f). ** indicates significant difference at $P \leq 0.01$ (Student's t test).

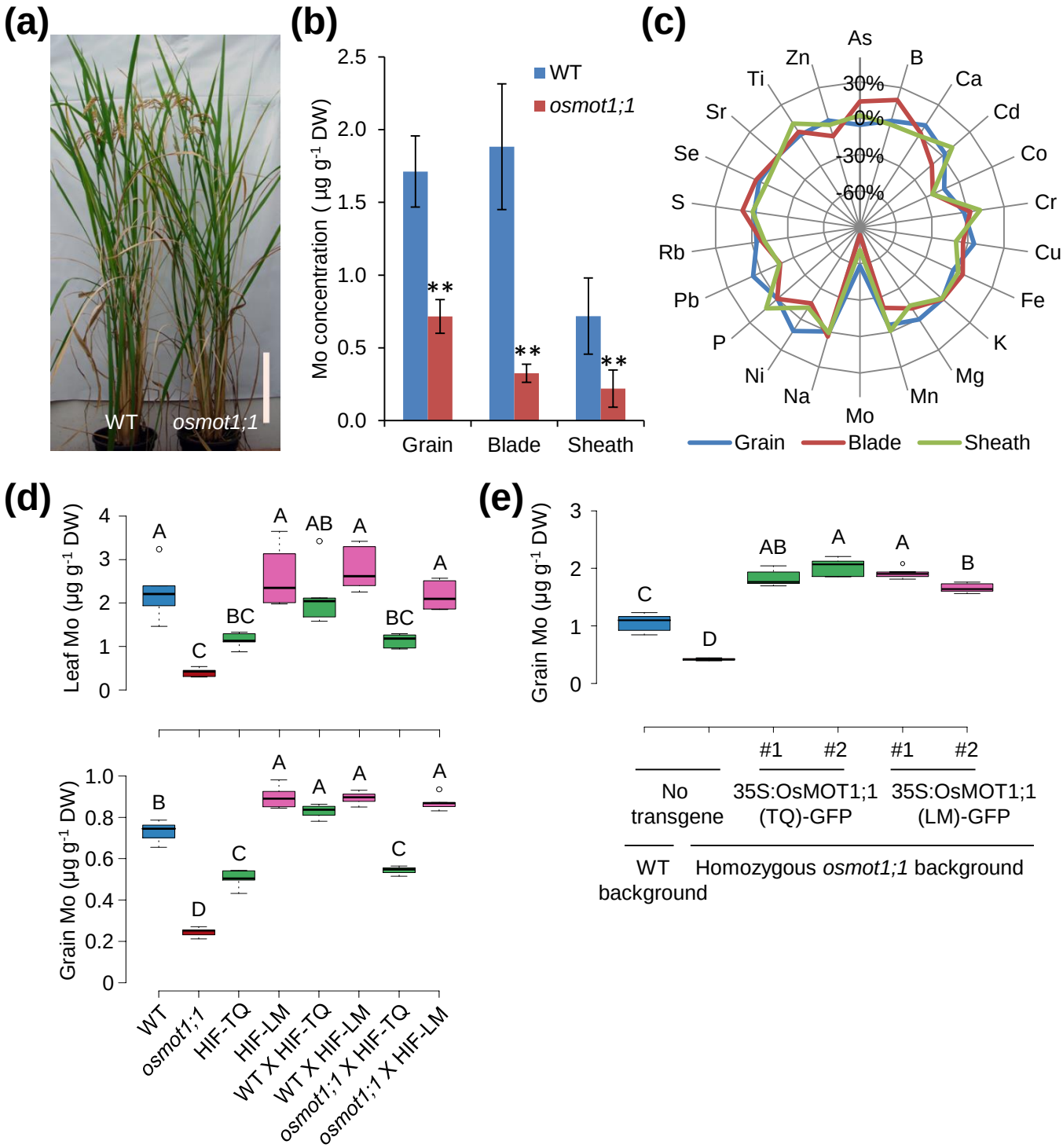

Fig 2. **Characterization of the *osmot1;1* mutant and complementation test.**
(a) Greenhouse grown WT and *osmot1;1* plants grown at harvesting stage. (b) Mo concentrations in the grain, blade and sheath of WT and *osmot1;1*. Data are presented as means ± SD (n = 8). ** indicates significant difference between WT and *osmot1;1* at $P \leq 0.01$ (Student's t test). (c) Percentage difference of 22 elements in the grain, blade and sheath of *osmot1;1* compared with the WT. Data are visualized in the radar chart. (d) Genetic complementation of *osmot1;1* by crossing with HIF669.4-TQ or HIF669.4-LM. The Mo concentrations in the grain of F1 plants were determined. (e) Transgenic complementation of *osmot1;1* by crossing with *OsMOT1;1* overexpression lines. The grain Mo concentrations of F2 plants in a homozygous mutant background containing *35S:OsMOT1;1(TQ)-GFP* or *35S:OsMOT1;1(LM)-GFP* constructs were determined. Two independent complemented lines were used for crossing. Data in (d, e) are presented as boxplots (n = 6). Boxes with different letters indicate significant difference at $P \leq 0.01$ (Tukey's HSD test). DW, dry weight.

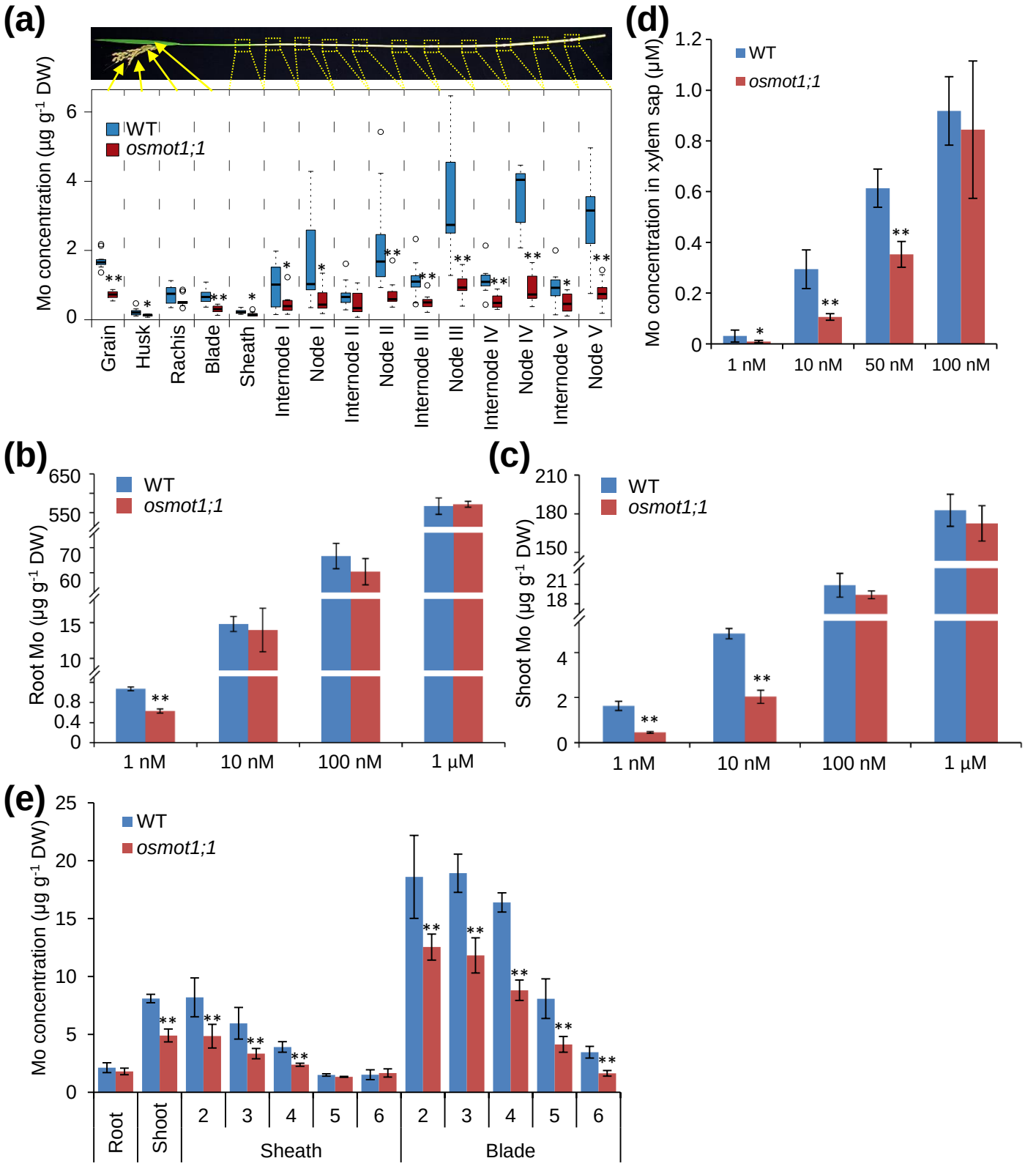
(a)
Mo concentration (µg g-1 DW)
WT
osmot1;1
Grain
Husk
Rachis
Blade
Sheath
Internode I
Node I
Internode II
Node II
Internode III
Node III
Internode IV
Node IV
Internode V
Node V
(d)
Mo concentration in xylem sap (µM)
WT
osmot1;1
1 nM
10 nM
50 nM
100 nM
(b)
Root Mo (µg g-1 DW)
WT
osmot1;1
1 nM
10 nM
100 nM
1 µM
(c)
Shoot Mo (µg g-1 DW)
WT
osmot1;1
1 nM
10 nM
100 nM
1 µM
(e)
Mo concentration (µg g-1 DW)
WT
osmot1;1
Root
Shoot
Sheath
Blade

Fig 3. **Low Mo phenotype of the *osmot1;1* mutant.**
(a) The Mo concentrations in different tissues of greenhouse grown WT and *osmot1;1* plants at harvesting stage. (b and c) The Mo concentrations in roots (b) and shoots (c) of WT and *osmot1;1*. Plants were hydroponically grown in nutrient solution containing various concentrations of Mo for two weeks. (d) The Mo concentration in the xylem sap of WT and *osmot1;1*. Plants were hydroponically grown in Mo-free nutrient solution for one week and treated with various concentrations of Mo for another week. (e) The Mo concentrations in different tissues of WT and *osmot1;1* seedlings. Plants were hydroponically grown in nutrient solution containing 10 nM of Mo for two weeks. Data (a) are presented as boxplots (n = 11 for WT and n = 10 for *osmot1;1*). Data in (b-e) are presented as means ± SD with n = 4 in (b and c), 8 in (d, e). * and ** indicate significant difference between WT and *osmot1;1* at $P \leq 0.05$ and 0.01 (Student's t test), respectively. DW, dry weight.

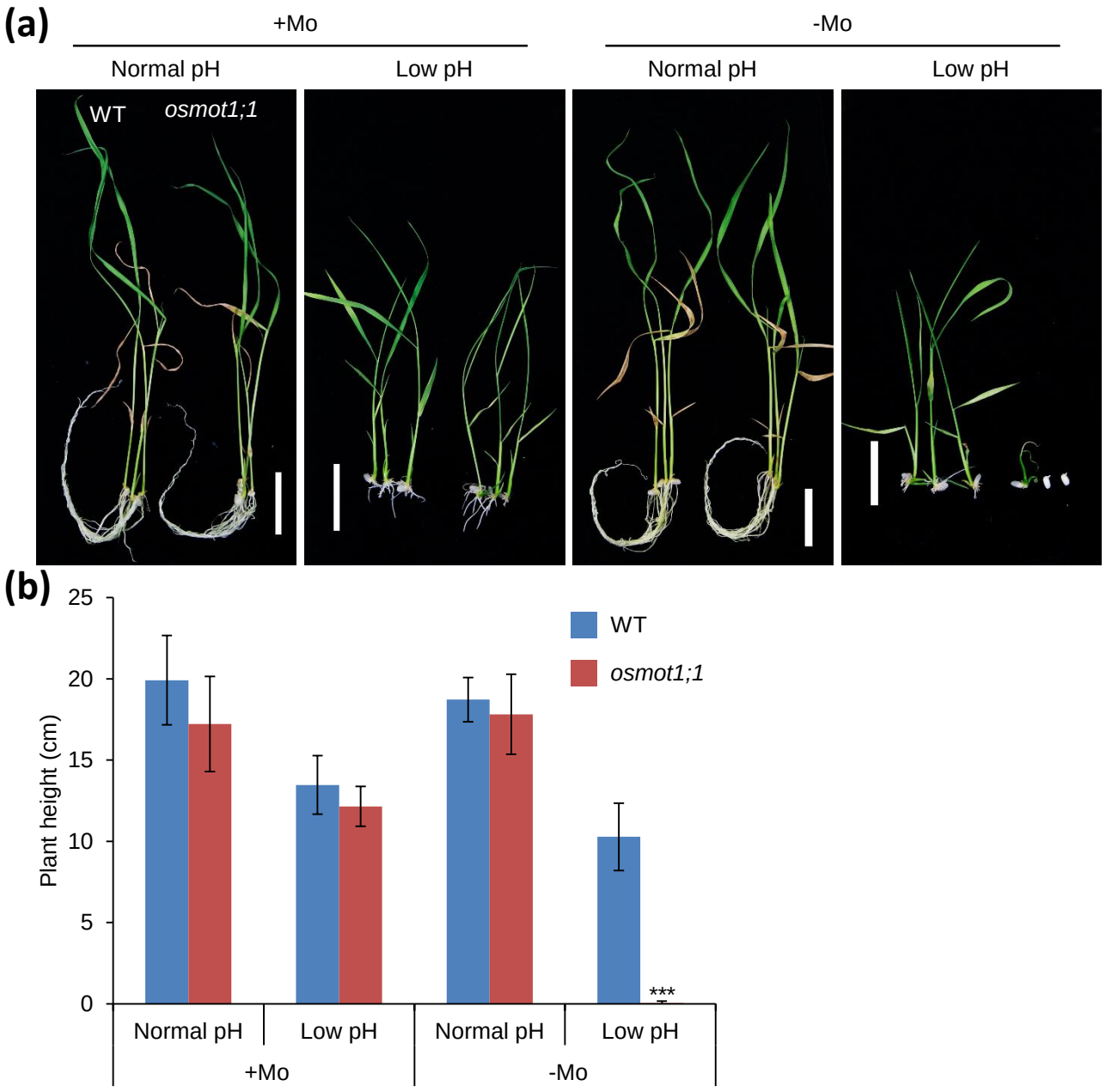

Fig 4. The *osmot1;1* mutant is sensitive to Mo deficiency at low pH condition.
(a) The phenotype of WT and *osmot1;1* grown under normal or low pH media with or without 1 μM Mo added. Low pH media was made by adding 50 μL 6 M HCl to 100 mL agar media after autoclaving. Plants were grown for 20 days. Bar, 3 cm. (b) The plant height of WT and *osmot1;1* grown as in (A). Data are presented as means ± SD with $n = 6$. *** indicated significant difference between WT and *osmot1;1* at $P \leq 0.001$ (Student's *t* test).

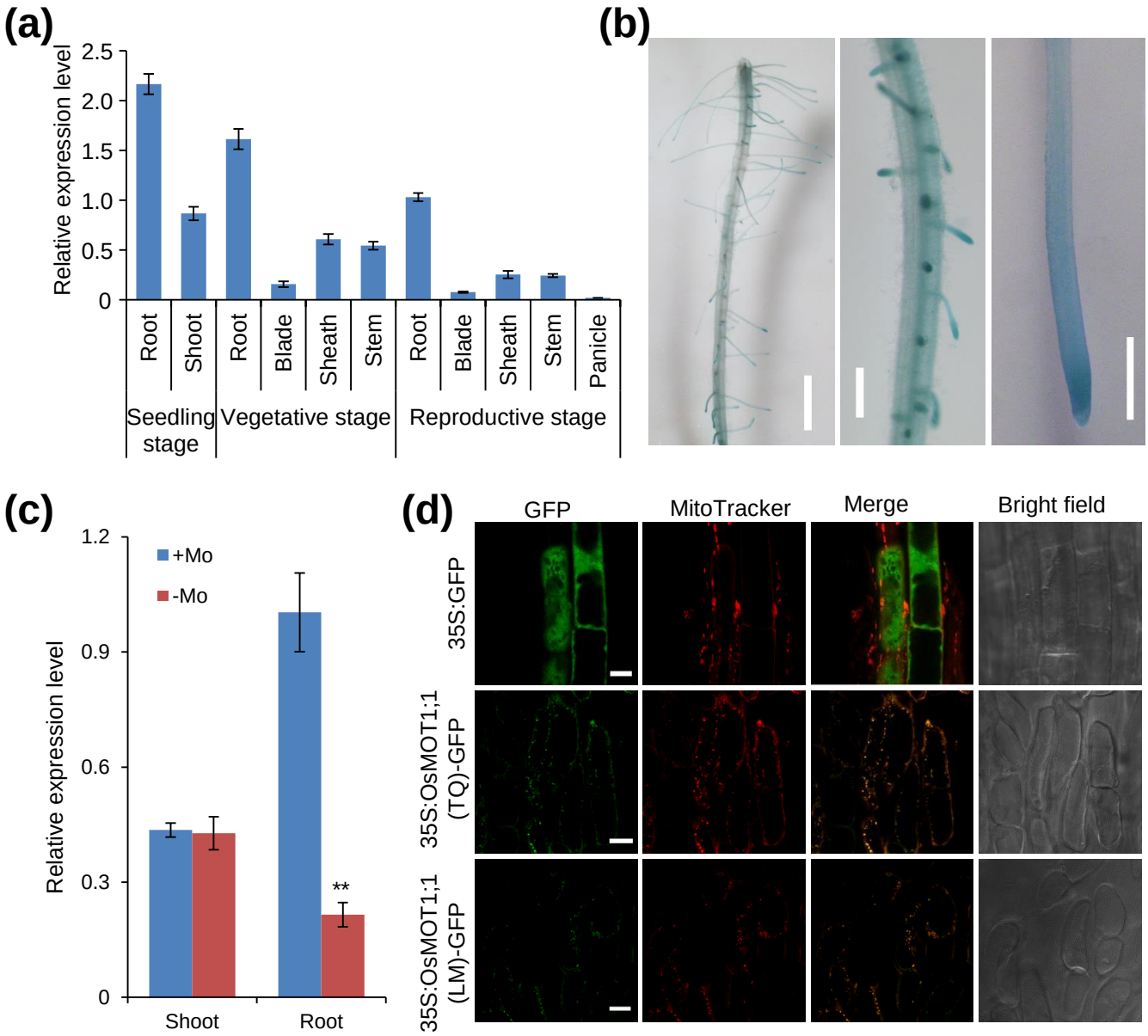

Fig 5. **Expression pattern and subcellular localization of OsMOT1;1**.
(a) Expression level of *OsMOT1;1* in different organs of Lemont at different growth stages. (b) Histochemical GUS staining of roots of transgenic rice plants transformed with *OsMOT1;1* promoter driven GUS constructs. The mature zone (left), elongation zone (middle) and root tip (right) of roots of 2-week-old plants are showed. Scale bars from left to right are 2, 0.5 and 2 mm. (c) Expression of *OsMOT1;1* was suppressed in roots under Mo deficiency. Lemont (LM) plants were grown hydroponically with 1 μM Mo for one week and then treated with 1 μM Mo (+Mo) or without Mo (-Mo) for another week. Relative expression level of was determined by qRT-PCR with three biological replicates. ** indicates significant difference at $P \leq 0.01$ (Student's *t* test). (d) Subcellular localization of OsMOT1;1 in stable transgenic rice plants. OsMOT1;1 from TeQing (TQ) or LM were fused with GFP at N-terminal and overexpressed under the control of CaMV 35S promoter. Mitochondria were stained with the specific dye MitoTracker. Scale bar, 10 μm.

Fig 6

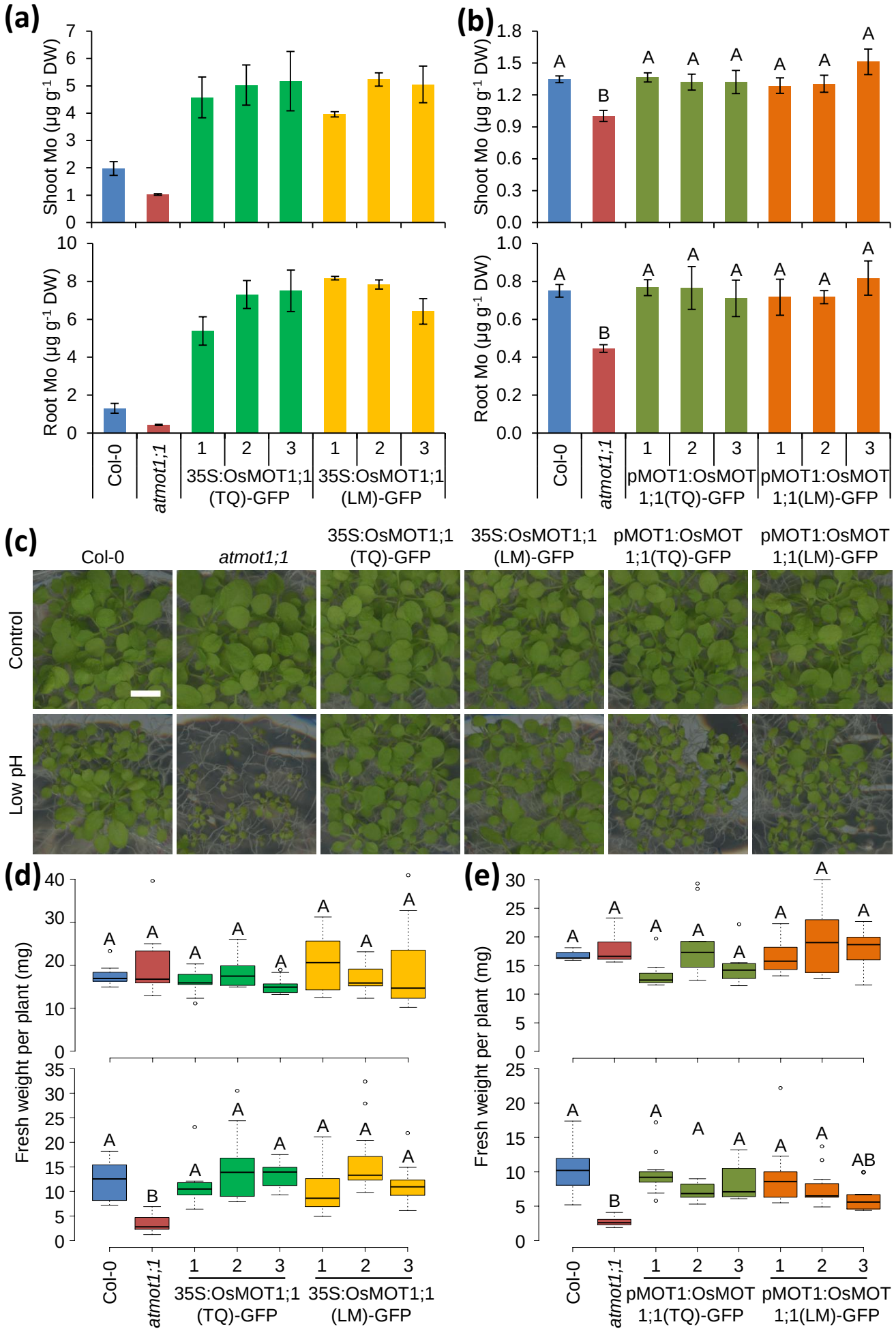
(a)
Shoot Mo (μg g-1 DW)
Root Mo (μg g-1 DW)
Col-0
atmot1;1
1
2
3
35S:OsMOT1;1 (TQ)-GFP
35S:OsMOT1;1 (LM)-GFP
(b)
Shoot Mo (μg g-1 DW)
Root Mo (μg g-1 DW)
pMOT1:OsMOT 1;1(TQ)-GFP
pMOT1:OsMOT 1;1(LM)-GFP
(c)
Col-0
atmot1;1
35S:OsMOT1;1 (TQ)-GFP
35S:OsMOT1;1 (LM)-GFP
pMOT1:OsMOT 1;1(TQ)-GFP
pMOT1:OsMOT 1;1(LM)-GFP
Control
Low pH
(d)
Fresh weight per plant (mg)
(e)
Fresh weight per plant (mg)

Fig 6 continued

Fig 6. **Functional analysis of *OsMOT1;1* in *Arabidopsis atmot1;1* mutant.**
(a and b) Mo concentrations in roots and shoots of the *mot1* mutant transformed with *OsMOT1;1-GFP* from TeQing (TQ) or Lemont (LM) driven by CaMV 35S promoter (a) or *AtMOT1;1* native promoter (b). Plants were grown on MGRL media containing 24 nM Mo for two weeks. Three independent transgenic lines are shown. (c) Phenotype of *OsMOT1;1-GFP* transgenic lines in *mot1* background. Plants were grown on MGRL media without added Mo at control or low pH condition for 20 days. Bar, 1 cm. (d and e) Fresh weight of *mot1* transformed with *OsMOT1;1-GFP* from TeQing (TQ) or Lemont (LM) driven by CaMV 35S promoter (d) or *AtMOT1;1* native promoter (e). Plants were grown as in (c). Three independent transgenic lines are shown. Data in (a) and (b) are shown as means ± SD with three biological replicates. Six plants were combined in each replicate. Data in (d) and (e) are shown as boxplots with n = 7 to 12. Columns or boxplots with different letters in (a) to (e) indicate significant difference at $P \leq 0.01$ (Tukey's HSD test). DW, dry weight.

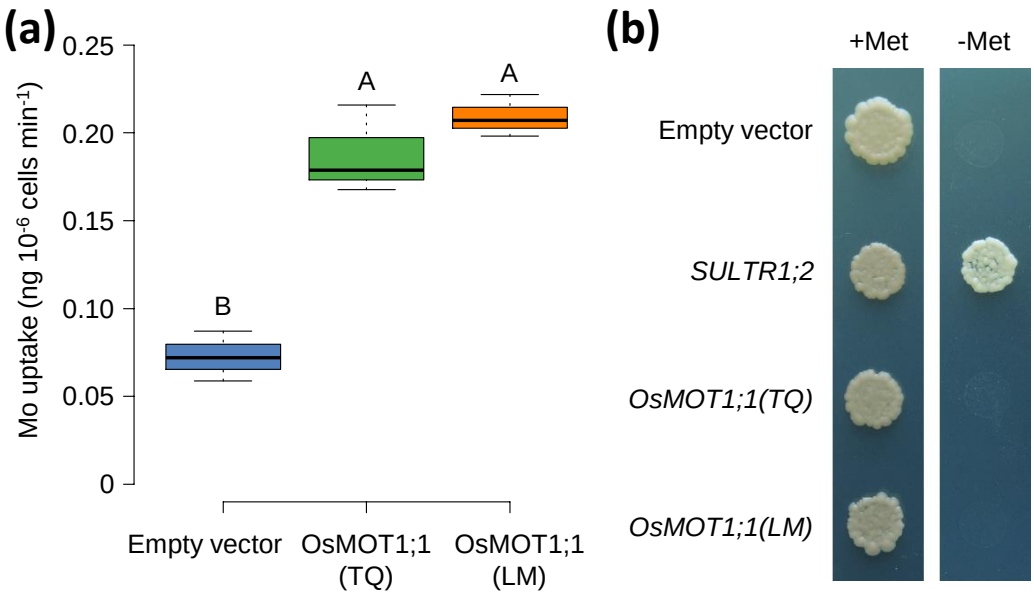

Fig 7. **Functional analysis of *OsMOT1;1* in yeast.**
(a) Molybdate transport activity of OsMOT1;1. Yeast strains transformed with empty vector, or *OsMOT1;1* from TeQing (TQ) or Lemont (LM) were incubated in media containing 0.5 μM Mo for 30 min. Mo concentrations in yeast cells were determined. Data are shown as boxplot with $n = 3$. Boxplots with different letters indicate significant difference at $P \leq 0.01$ (Tukey's HSD test). (b) Complementation analysis of a yeast mutant defective in sulfate uptake. The yeast mutant strains transformed with empty vector, *SULTR1;2*, or *OsMOT1;1* from TQ or LM were incubated on media containing 0.5 mM sulfate with or without added Met for four days.

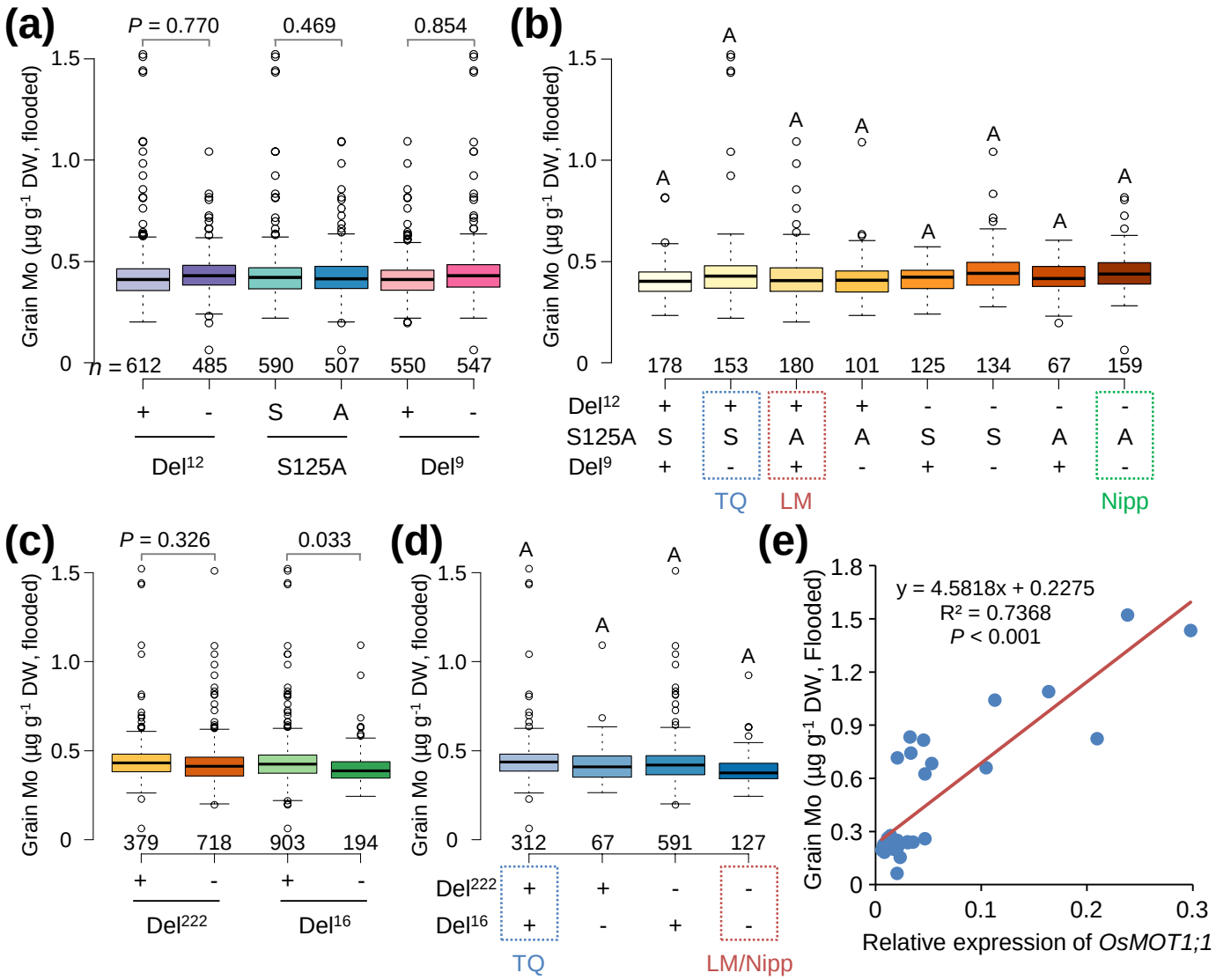

Fig 8. Contribution of allelic variation of *OsMOT1;1* on the variation of grain Mo in USDA rice core collection grown in flooded condition.

(a) The grain Mo in rice accessions with different alleles at three polymorphic sites in the coding region of *OsMOT1;1*. (b) The grain Mo in rice accessions with different haplotypes derived from the combination of three polymorphic sites in the coding region of *OsMOT1;1*. (c) The grain Mo in rice accessions with or without the deletions in the promoter region of *OsMOT1;1*. (d) The grain Mo in rice accessions with different promoter haplotypes derived from the combination of two deletions in the coding region of *OsMOT1;1*. Data in (a - d) are shown as boxplots. Numbers under the boxes are the accession number; numbers above the boxes are the *P* values; the same letters above the boxes indicate no significant difference at $P \leq 0.01$ (Tukey's HSD test). + and – represent the presence and absence of the deletion, respectively. The dash color boxes in (b) and (d) mark the haplotypes in TQ , LM and Nipp. (e) The correlation of the relative expression of *OsMOT1;1* in roots with the grain Mo concentration in 35 rice accessions grown in flooded condition. The expression of *OsMOT1;1* in the roots of 3-week-old plants were determined by qRT-PCR. The relative expression level of *OsMOT1;1* was normalized the rice actin gene, and presented as the mean of 2^(-deltaCt) with three biological replicates.